Synthesis and Characterization of New Ruthenium−Iridium Mixed-Metal Clusters. Crystal Structures of $[Ru_3IrH_3(CO)_{11}(PPh_3)]$, $[Ru_3IrH(CO)_{12}(PPh_3)]$, and $[Ru_{4-x}Ir_xH_{4-x}(CO)_{10}(PPh_3)_2]$ (x = 1 and 2)

Aapo U. Härkönen, Markku Ahlgrén, and Tapani A. Pakkanen*

Department of Chemistry, University of Joensuu, P.O. Box 111, FIN-80101 Joensuu, Finland

Jouni Pursiainen

Department of Chemistry, University of Oulu, Linnanmaa, FIN-90571 Oulu, Finland

Received June 3, 1996[⊗]

The study of reactions between $[Ir(CO)Cl(PPh_3)_2]$ and $Na[Ru_3H(CO)_{11}]$ in different solvents yields a rich source of new mixed-metal Ru−Ir clusters. New ruthenium−iridium mixed-metal clusters $[Ru_3IrH_3(CO)_{11}(PPh_3)]$ (two isomers), $[Ru_3IrH(CO)_{12}(PPh_3)]$, and $[Ru_{4-x}Ir_xH_{4-x}(CO)_{10}(PPh_3)_2]$ (x = 1 and 2) were synthesized and characterized by ^1H and ^{31}P NMR and infrared spectroscopy and by single-crystal X-ray structure determination.

Introduction

Mixed-metal cluster compounds have attracted much attention during the last few decades,[1] particularly the mixed-metal clusters of the iron and cobalt groups.[2] In view of this, it is somewhat surprising that only a few examples of closed tetranuclear Ru−Ir clusters are known. Structural information is available only for one anionic cluster, $[RuIr_3(CO)_{12}]^-$,[3] and for the phosphine complex $[Ru_3IrH_2(CO)_8(PPh_3)(\mu\text{-}PPh_2)(PPhC_6H_4)]$.[4] Only three Ru−Ir mixed-metal clusters that are not tetranuclear are known, namely, $[RuIr_4(CO)_{15}]^{2-}$ [3] and the $[N(PPh_3)_2][trans\text{-}Ru_4Ir_2(CO)_{16}B]$[5] and $cis\text{-}[Ru_4Ir_2(CO)_{16}B(\mu\text{-}AuP(C_6H_{11})_3)]$ cages.[5]

We carried out reactions between $[Ir(CO)Cl(PPh_3)_2]$ and $Na[Ru_3H(CO)_{11}]$ in different solvents, which are shown to be a rich source of new mixed-metal Ru−Ir clusters. The clusters $[Ru_3IrH_3(CO)_{11}(PPh_3)]$ (two isomers), $[Ru_3IrH(CO)_{12}(PPh_3)]$, and $[Ru_{4-x}Ir_xH_{4-x}(CO)_{10}(PPh_3)_2]$ (x = 1 and 2), which we now report, were characterized by ^1H and ^{31}P NMR and infrared spectroscopy and by single-crystal X-ray structure determination.

Results and Discussion

The reaction of $[Ir(CO)Cl(PPh_3)_2]$ and $Na[Ru_3H(CO)_{11}]$ (molar ratio ca. 1:1) in tetrahydrofuran (THF) at room temperature led to the formation of $[Ru_3(CO)_{12}]$ and to several Ru−Ir mixed-metal cluster compounds showing strikingly similar spectroscopic and structural properties. As we have reported earlier, small amounts of Ru_4 clusters are also formed in the reaction.[6] The product distribution varied depending on the solvent. Scheme 1 illustrates the formation of the new Ru−Ir species **1**−**5**, together with three known Ru species which were also identified. Compounds **4** and **5** crystallized together.

Data for the Synthesis of Compounds 1−5. The reaction between $[Ir(CO)Cl(PPh_3)_2]$ and $Na[Ru_3H(CO)_{11}]$ produced the clusters **1**−**5** together with two Ru_4 clusters and $[Ru_3(CO)_{12}]$. Compounds were produced in different amounts according to the solvent. Compound **1** formed under all reaction conditions, independent of the solvent, but in different yields. Compound **2** formed under all reaction conditions except under hydrogen atmosphere. Compound **3** formed only in THF but not in THF under hydrogen atmosphere. All reactions yielded compounds **4** and **5**. Furthermore, the reaction under hydrogen produced $[Ru_4H_4(CO)_{11}(PPh_3)]$, which was identified from IR and ^1H NMR spectral data.[7] Another Ru_4 cluster formed only in THF and was chararcterized as $[Ru_4H_2(CO)_{12}(PPh_3)]$ by spectroscopic methods.[6] Since its IR spectrum was almost identical with that of **2**, with a bridging carbonyl signal, probably also the structures of $[Ru_4H_2(CO)_{12}(PPh_3)]$ and **2** are similar. All reactions produced some $[Ru_3(CO)_{12}]$ and minor amounts of other unidentified cluster compounds. Production of the clusters under the different reaction conditions is shown in Table 3.

Solid-State Structures of 1−5. The crystal structure of $[Ru_3IrH_3(CO)_{11}(PPh_3)]$ (**1**), with the labeling scheme, is shown in Figure 1, and the relevant bond distances and angles appear in Tables 4 and 5 for all the compounds. The metal skeleton of **1** is based on a Ru_3Ir tetrahedron, where the phosphine ligand is coordinated to an axial position of the Ru(2) atom in

[⊗] Abstract published in *Advance ACS Abstracts,* February 1, 1997.

(1) Adams, R. D. In *Comprehensive Organometallic Chemistry*; Abel, E. W., Stone, F. G. A., Wilkinson, G., Eds.; Pergamon Press: Oxford, U.K., 1995; Vol. 10, Chapter 1.
(2) Pakkanen, T. A.; Pursiainen, J.; Venäläinen, T.; Pakkanen, T. T. *J. Organomet. Chem.* **1989**, *372*, 129.
(3) Fumagalli, A.; Demartin, F.; Sironi, A. *J. Organomet. Chem.* **1985**, *279*, C33.
(4) Jungbluth, H.; Süss-Fink, G.; Pellinghelli, M. A.; Tiripicchio, A. *Organometallics* **1990**, *9*, 1670.
(5) Galsworthy, J. R.; Hattersley, A. D.; Housecroft, C. E.; Rheingold, A. L.; Waller, A. *J. Chem. Soc., Dalton Trans.* **1995**, 549.
(6) Härkönen, A. U.; Ahlgrén, M.; Pakkanen, T. A.; Pursiainen, J. *J. Organomet. Chem.* **1997**, in press.
(7) Piacenti, F.; Bianchi, M.; Frediani, P.; Benedetti, E. *Inorg. Chem.* **1971**, *10*, 2759.

S0276-7333(96)00432-3 CCC: $14.00

Scheme 1

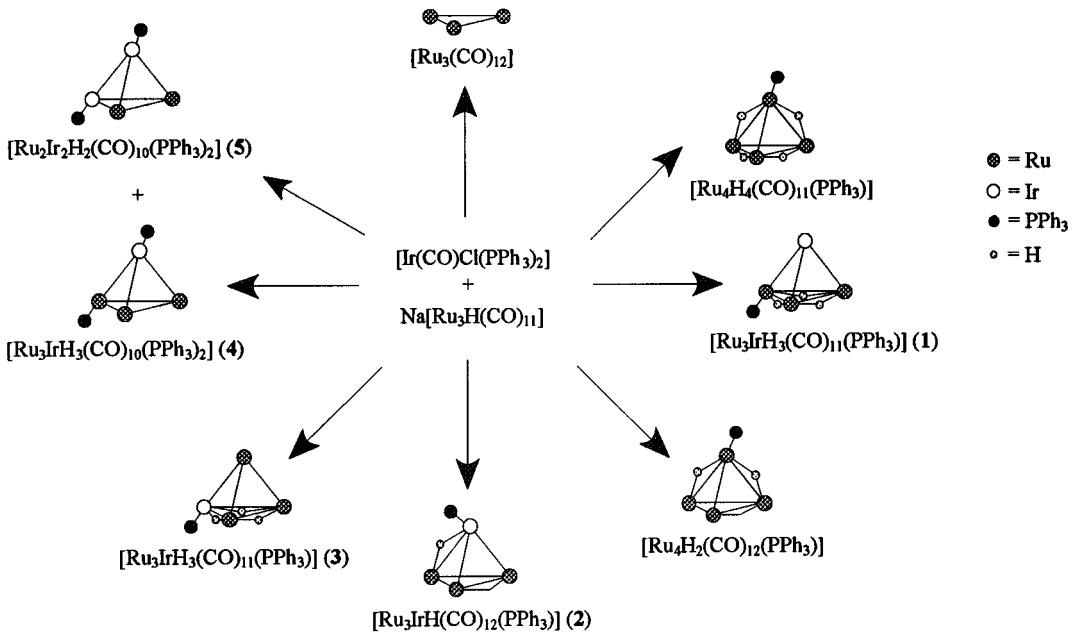

Table 1. Infrared Data for Compounds 1−5

formula	no.	solvent	ν(CO), cm^{-1}
$Ru_3IrH_3(CO)_{11}(PPh_3)$	**1**	*n*-hexane	2095 w, 2069 w, 2048 s, 2031 m, 2026 m, 2016 s, 1988 w
$Ru_3IrH(CO)_{12}(PPh_3)$	**2**	*n*-hexane	2086 m, 2049 vs, 2042 vs, 2031 s, 2009 m, 2000 m, 1877 w
$Ru_3IrH_3(CO)_{11}(PPh_3)$	**3**	*n*-hexane	2089 w, 2068 s, 2054 m, 2048 s, 2037 m, 2024 s, 2005 m, 1985 w, 1961 w
$Ru_{4-x}Ir_xH_{4-x}(CO)_{10}(PPh_3)_2$ (x = 1, 2)	**4** and **5**	*n*-hexane	2073 s, 2041 vs, 2023 vs, 2018 s, 1996 w, 1983 m, 1960 w

Table 2. ^{1}H NMR Data for Compounds 1−5

formula	no.	solvent	$\delta(\mu_2$-H), ppm[a]
$Ru_3IrH_3(CO)_{11}(PPh_3)$	**1**	$CDCl_3$	7.43 m, −16.9 dd, −17.9 t (−60 → 20 °C)
$Ru_3IrH(CO)_{12}(PPh_3)$	**2**	$CDCl_3$	7.44 m, −18.4 d (−60 → 20 °C)
$Ru_3IrH_3(CO)_{11}(PPh_3)$	**3**	$CDCl_3$	7.49 m, −17.9 s (20 °C)
		toluene-d_8	7.53 s, 7.45 s, 7.37 s, −15.2 br, −16.6 s, −17.7 br, −19.1 d, −21.0 br (−80 °C)
$Ru_{4-x}Ir_xH_{4-x}(CO)_{10}(PPh_3)_2$ (x = 1, 2)	**4** and **5**	$CDCl_3$	7.32 br, −16.4 br, −17.1 br (20 °C)
		$CDCl_3$	7.43 m, −16.2 d, −16.5 br, −17.9 d (−55 °C)

[a] Spectra observed at 250 MHz.

Table 3. Production of the Clusters under Different Reaction Conditions

compound	THF (%)	THF[a] (%)	THF[b] (%)	*n*-hexane[c] (%)	CH_2Cl_2 (%)
$[Ru_3(CO)_{12}]$	45	35	46	58	22
1	7	15	13	21	11
2	<5	17		7	13
3	7	9	10		
4 and **5**	32	21	23	11	<5
$[Ru_4H_4(CO)_{11}(PPh_3)]$			7		
$[Ru_4H_2(CO)_{12}(PPh_3)]$	<5				

[a] Reaction with acidification. [b] Reaction in hydrogen with acidification. [c] Reaction with reflux.

the Ru_3 basal triangle. Eleven terminal carbonyl ligands and three Ru−H−Ru hydrides complete the structure. The Ru−Ru distances average 2.944 Å and compare well with the hydride-bridged Ru−Ru distances found in other clusters.[2,8] The arrangement of the ligands in compound **1** is similar to that in $[Ru_3RhH_3(CO)_{12}]$[8] and $[Ru_3CoH_3(CO)_{12}]$.[9] The average values for Ru−Ru−CO_{ax} angles are 114.6° for $[Ru_3IrH_3(CO)_{11}(PPh_3)]$, 113.9° for $[Ru_3RhH_3(CO)_{12}]$, and 114.5° for $[Ru_3CoH_3(CO)_{12}]$. For angles M−Ru−CO_{eq} (M = Ir, Rh, Co), the values

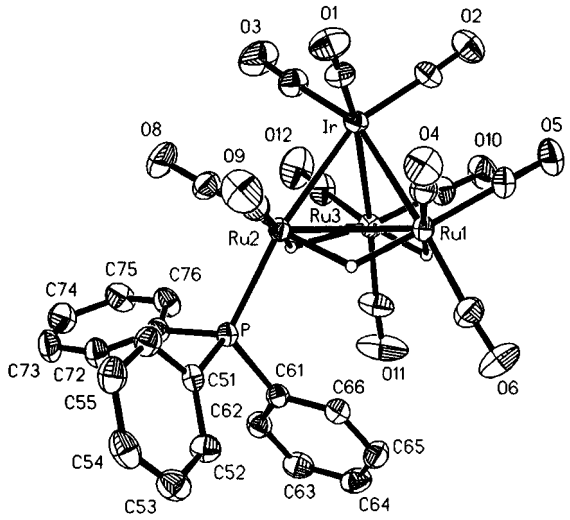

Figure 1. Molecular structure of $[Ru_3IrH_3(CO)_{11}(PPh_3)]$ (**1**) with the atom-labeling scheme. The thermal ellipsoids are drawn at the 35% probability level. The hydrogen atoms, except those bound to metal−metal edges, have been omitted for clarity.

are 92.1° for $[Ru_3IrH_3(CO)_{11}(PPh_3)]$, 91.4° for $[Ru_3RhH_3(CO)_{12}]$, and 92.4° for $[Ru_3CoH_3(CO)_{12}]$.

The structure of $[Ru_3IrH(CO)_{12}(PPh_3)]$ (**2**) is presented in Figure 2, together with the numbering scheme. The

(8) Pursiainen, J.; Pakkanen, T. A. *J. Chem. Soc., Dalton Trans.* **1989**, 2449.
(9) Gladfelter, W. L.; Geoffroy, G. L.; Calabrese, J. C. *Inorg. Chem.* **1980**, *19*, 2569.

Table 4. Metal−Metal Bond Lengths (Å) for Compounds 1−5

	1	2	3	4 and 5
Ir−Ru(1)	2.759(1)	2.822(1)	2.927(1)	2.938(1)
Ir−Ru(2)	2.758(1)	2.938(1)	2.919(1)	2.983(1)[a]
Ir−Ru(3)	2.741(1)	2.744(1)	2.789(1)	2.799(1)
Ru(1)−Ru(2)	2.936(1)	2.758(1)	2.900(1)	2.807(1)[a]
Ru(1)−Ru(3)	2.922(1)	2.802(2)	2.760(1)	2.746(2)
Ru(2)−Ru(3)	2.975(1)	2.794(1)	2.757(1)	2.924(1)[a]
Ir−C(1)/P/P(1)	1.909(5)	2.370(2)	2.379(2)	2.372(3)
Ir−C(2)	1.926(6)	1.864(9)	1.904(6)	1.876(11)
Ir−C(3)	1.901(6)	1.918(9)	1.877(7)	1.925(12)
Ru(1)−C(4)	1.917(5)	1.920(10)	1.936(9)	1.890(2)
Ru(1)−C(5)	1.915(6)	1.921(10)	1.894(8)	1.870(2)
Ru(1)−C(6)	1.917(6)	1.911(10)	1.880(7)	1.860(2)
Ru(2)−P/C(7)	2.370(2)	1.875(9)	1.873(7)	1.871(12)[a]
Ru(2)−C(8)/P(2)	1.873(6)	1.898(12)	1.875(7)	2.374(3)[a]
Ru(2)−C(9)	1.890(6)	1.929(11)	1.934(7)	1.874(11)[a]
Ru(3)−C(10)	1.924(6)	1.920(11)	1.894(9)	1.889(13)
Ru(3)−C(11)	1.932(6)	1.928(11)	1.854(6)	1.879(12)
Ru(3)−C(12)	1.882(6)	1.898(13)	1.890(9)	1.910(2)
Ru(1)−C(13)		2.110(10)		
Ru(3)−C(13)		2.192(11)		

[a] Ru(2) corresponding M atom occupation $Ru_{0.54}Ir_{0.46}$.

Table 5. Selected Bond Angles (deg) for Compounds 1−5

	1	2	3	4 and 5
Ir−Ru(1)−C(4)	91.3(2)	92.6(3)	110.8(2)	116.3(4)
Ir−Ru(1)−C(5)	87.9(2)	98.5(3)	97.4(2)	102.9(5)
Ir−Ru(2)−C(8)/P(2)	90.9(2)	110.2(4)	96.6(2)	112.4(7)[a]
Ir−Ru(2)−C(9)	97.8(2)	111.1(3)	120.3(2)	102.8(3)[a]
Ir−Ru(3)−C(10)	92.3(2)	98.9(3)	99.8(2)	96.3(4)
Ir−Ru(3)−C(12)	92.4(2)	87.2(4)	102.4(2)	102.0(4)
Ru(2)−Ru(1)−C(4)	95.5(1)	69.4(3)	114.2(2)	98.9(4)[a]
Ru(3)−Ru(1)−C(4)	147.4(2)	129.0(3)	168.7(2)	162.3(4)
Ru(2)−Ru(1)−C(5)	144.8(2)	155.0(3)	144.3(3)	162.8(5)[a]
Ru(3)−Ru(1)−C(5)	95.3(2)	126.9(3)	86.7(3)	101.9(5)
Ru(1)−Ru(2)−C(8)/P(2)	148.8(2)	156.7(5)	149.4(2)	172.7(7)[a]
Ru(3)−Ru(2)−C(8)/P(2)	105.4(2)	96.1(5)	93.2(2)	117.2(7)[a]
Ru(1)−Ru(2)−C(9)	94.2(2)	111.2(3)	113.8(3)	87.1(3)[a]
Ru(3)−Ru(2)−C(9)	149.7(2)	167.6(3)	172.0(2)	143.7(3)[a]
Ru(1)−Ru(3)−C(10)	94.8(2)	119.0(4)	102.7(3)	85.3(4)
Ru(2)−Ru(3)−C(10)	147.2(2)	162.2(3)	161.4(3)	143.7(4)[a]
Ru(1)−Ru(3)−C(12)	150.2(2)	138.1(4)	158.5(2)	165.7(4)
Ru(2)−Ru(3)−C(12)	101.7(2)	83.4(4)	96.1(2)	118.3(4)[a]
Ru(1)−Ru(2)−P/C(7)	117.2(1)	87.7(3)	93.9(2)	87.7(4)[a]
Ru(3)−Ru(2)−P/C(7)	106.7(1)	91.7(3)	82.8(2)	92.9(4)[a]
Ru(2)−Ru(1)−C(6)	119.1(2)	103.4(3)	95.7(2)	96.5(4)[a]
Ru(3)−Ru(1)−C(6)	115.6(2)	107.1(3)	92.8(3)	85.6(5)
Ru(1)−Ru(3)−C(11)	111.9(2)	106.4(3)	97.0(3)	100.3(5)
Ru(2)−Ru(3)−C(11)	111.9(2)	95.9(3)	101.7(2)	97.9(4)[a]
Ru(1)−Ir−C(1)/P/P(1)	95.1(2)	111.7(6)	111.8(1)	119.2(7)
Ru(2)−Ir−C(1)/P/P(1)	92.9(2)	111.0(5)	115.3(1)	112.5(7)[a]
Ru(1)−Ir−C(2)	98.5(2)	84.1(3)	96.1(2)	91.3(4)
Ru(3)−Ir−C(2)	96.6(2)	86.0(3)	86.0(2)	88.2(3)
Ru(2)−Ir−C(3)	95.4(2)	107.9(3)	90.4(2)	100.3(3)[a]
Ru(3)−Ir−C(3)	96.2(2)	96.7(3)	85.9(2)	83.4(3)
Ru(1)−C(13)−Ru(3)		81.3(4)		

[a] Ru(2) corresponding M atom occupation $Ru_{0.54}Ir_{0.46}$.

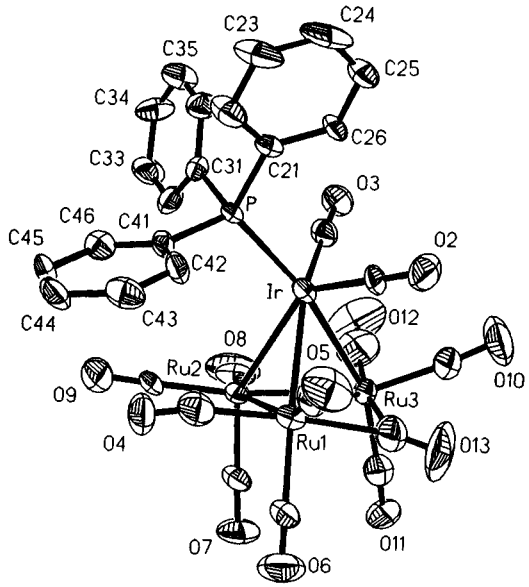

Figure 2. Molecular structure of $[Ru_3IrH(CO)_{12}(PPh_3)]$ (**2**) with the atom-labeling scheme. The thermal ellipsoids are drawn at the 35% probability level. The hydrogen atom μ_2-bonded to the Ru−Ir edge was not located by X-ray methods, and all other hydrogen atoms have been omitted for clarity.

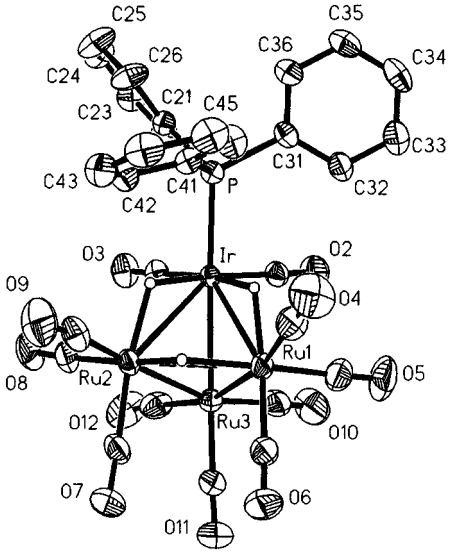

Figure 3. Molecular structure of $[Ru_3IrH_3(CO)_{11}(PPh_3)]$ (**3**) with the atom-labeling scheme. The thermal ellipsoids are drawn at the 35% probability level. The hydrogen atoms, except those bound to metal−metal edges, have been omitted for clarity.

structure of **2** differs from that of compound **1** in having one bridging carbonyl ligand and only one hydride ligand. The hydrogen atom was not located crystallographically. Inspection of the geometry of the carbonyl ligands and metal−metal bond lengths, as well as the ^{1}H NMR data (^2J(P−H) = 9.6 Hz), suggest bonding on the Ru(2)−Ir edge. The apical phosphine ligand is now coordinated to the Ir atom. The valence isoelectronic molecule **2** can be compared with the crystal structure of $[Ru_4H_2(CO)_{12}(PPh_3)]$,[6] which we have recently reported. While both clusters have one Ru(μ_2-CO)Ru bridging carbonyl, the relative sites of the phosphine ligands are different. This is evidently due to the steric and electronic requirements of the second hydride ligand in $[Ru_4H_2(CO)_{12}(PPh_3)]$.

The crystal structure determination revealed that compound **3**, $[Ru_3IrH_3(CO)_{11}(PPh_3)]$, is a structural isomer of compound **1**. The complexity of the infrared spectrum and the observed low-temperature ^{1}H NMR spectrum of $[Ru_3IrH_3(CO)_{11}(PPh_3)]$ (**3**) show two isomers of compound **3** to be present in solution (see below). The crystal structure of **3** is shown in Figure 3. In the solid-state structure of **3** the phosphine ligand is coordinated apically to the Ir atom, in contrast to compound **1** where the axial phosphine is coordinated to the Ru atom. The three hydride ligands were located by difference Fourier techniques and found to bridge the two Ru−Ir bonds and one Ru−Ru bond in the Ru_2Ir triangle. We could

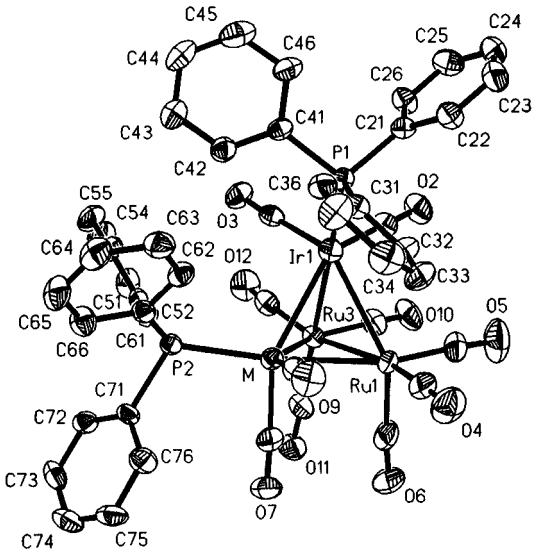

Figure 4. Molecular structure of $[Ru_{4-x}Ir_xH_{4-x}(CO)_{10}(PPh_3)_2]$ ($x = 1$ (**4**) and 2 (**5**)) with the atom-labeling scheme. The thermal ellipsoids are drawn at the 35% probability level. The site occupation factor of iridium refined to 46% for metal atom M. The hydrogen atoms μ_2-bonded to the Ru−Ru and Ru−Ir edges were not located by X-ray methods, and all other hydrogen atoms have been omitted for clarity.

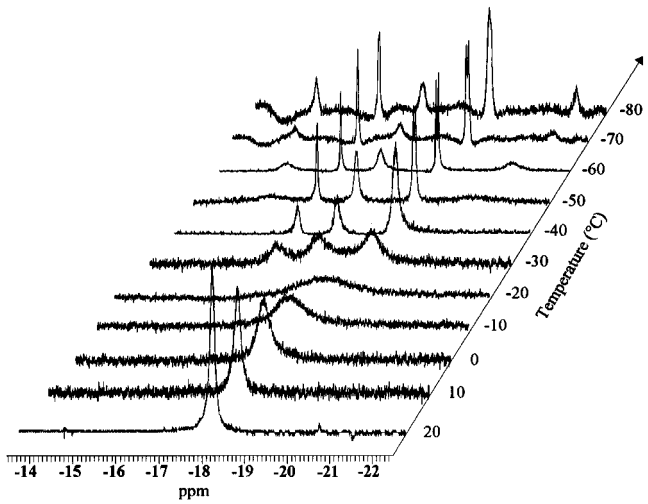

Figure 5. 250-MHz ^{1}H NMR spectra of $[Ru_3IrH_3(CO)_{11}(PPh_3)]$ (**3**) in $CDCl_3$ solution.

see a clear stereochemical relationship, if we orientate **3** to the same position as **1** in Figure 1. In that case we observed for **3** that the three bridging hydrides are not coplanar with the Ru_2Ir triangle but lie below it as illustrated for **1** in Figure 1.

Comparison of the carbonyl geometries of **1** and **3** (Figures 1 and 3) shows that, relative to **1**, the apical carbonyls of **3** are significantly more inclined downward from the apical metal. As compared with the carbonyls and Ru_3 basal plane of cluster **3**, the equatorial carbonyls in **1** are bent up from the Ru_3 basal plane and, correspondingly, the axial carbonyls CO(6) and CO(11) are bent slightly away from it.

The crystal structure of the solid solution of complex $[Ru_{4-x}Ir_xH_{4-x}(CO)_{10}(PPh_3)_2]$ ($x = 1$ (**4**) and 2 (**5**)) is presented in Figure 4 together with the atom-numbering scheme. Refinement of the occupancy factor for the atom M at the M site gave $Ru_{0.54}Ir_{0.46}$. Phosphine ligands are coordinated apically to the Ir atom and equatorially to the M atom. Axial carbonyls are significantly bent under the Ru_2M plane, and the equatorial carbonyls are nearly coplanar with the Ru_2M basal plane.

The coordination of the phosphine on ruthenium atom in **1** distinguishes this cluster from the tetranuclear Ru-Rh clusters, where Rh is exclusively preferred as the coordination site. The preference between ruthenium and cobalt is not clear since both Ru- and Co-coordinated phosphines have been found among Ru−Co clusters.[10,11] Since there are two isomers (**1** and **3**) with bonding of phosphines on Ru and Ir, there cannot be much difference in the coordination ability of Ru and Ir toward phosphines. The hydride and the phosphine tend to coordinate *cis* to each other, as observed in all structures **1**−**5**. Probably both steric and electronic factors contribute to the preferences in the coordination of the phosphine and hydride ligands.[12]

Cluster hydrides in the structural isomers of **1** and **3** were located by X-ray diffraction (see Figures 1 and 3). In **1**, the hydrogens prefer to bridge the Ru−Ru edge, as found previously in $[Ru_3RhH_3(CO)_{12}]$[8] and $[Ru_3CoH_3(CO)_{12}]$.[9] In **3**, two of the hydrogen atoms instead bridge Ru−Ir edges. The hydride in **2** was located on the basis of the bond lengths (Table 4) and bond angles (Table 5): the hydrogen-bridged bond Ir−Ru(2) was clearly longer than the other metal−metal bonds. In addition it was evident in the ^{1}H NMR spectrum that there is coupling of hydrogen to the phosphorus atom. In all three complexes the repulsion from the hydrogens can also be seen in the M(1)−M(2)−C bond angle data.

Spectroscopic Data for Compounds 1−5. The carbonyl infrared spectroscopic data were measured in *n*-hexane and are reported in the Experimental Section. The ^{1}H NMR spectrum of **1** at room temperature shows two signals, at −16.9 ppm (dd, ^2J(P−H) = 11.2 and 11.2 Hz) and −17.9 ppm (t, ^2J(H−H) = 2.9 Hz). No temperature dependence was observed (−60 to 30 °C). The ^{1}H NMR spectrum of **2** exhibits one signal at −18.4 ppm (d, ^2J(P−H) = 9.6 Hz), and as in **1**, no temperature dependence was observed.

The ^{1}H NMR spectrum of **3** at room temperature exhibits one broad singlet at −17.9 ppm. However, as shown in Figure 5, upon cooling of the solution to −30 °C the singlet develops into three separate broad peaks. Upon further cooling of the solution to −60 °C, altogether five separate peaks, at −15.2 (br), −16.6 (s), −17.7 (d, br), −19.1 (d, ^2J(P−H) = 14.1 Hz), and −21.0 (br) ppm, are developed, with relative intensities 0.61:1:1.05:2:0.53. At −60 °C the peaks at −15.2, −17.7, and −21.0 ppm are clearly broader than the peaks at −16.6 and −19.1 ppm. The low-temperature ^{1}H NMR pattern (Figure 5) shows two different isomeric forms of **3** (**3a**,**b** in Scheme 2) to be present in solution. One of these (**3a**) is isomer the structurally characterized in the solid state. The resonances at δ −16.6 and −19.1 ppm in the −60 °C ^{1}H NMR spectrum have an intensity ratio of 1:2, which suggests that they arise from a single isomer (**3a**) in which two of the hydrogens are equivalent (δ −19.1) but differ from the third (δ −16.6). The remain-

(10) Pursiainen, J.; Pakkanen, T. A. *J. Organomet. Chem.* **1986**, *309*, 187.

(11) Braunstein, P.; Rosé, J.; Toussaint, D.; Jääskeläinen, S.; Ahlgrén, M.; Pakkanen, T. A.; Pursiainen, J.; Toupet, L.; Grandjean, D. *Organometallics* **1994**, *13*, 2472.

(12) Benfield, R. E.; Johnson, B. F. G. *J. Chem. Soc., Dalton Trans.* **1980**, 1743−67.

Scheme 2

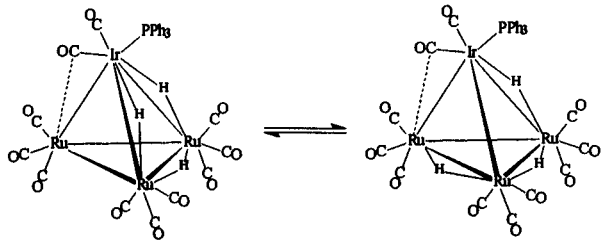

3a **3b**

ing three resonances, at −15.2, −17.7, and −21.0 ppm, are due to another isomer (**3b**) in which all three hydrogens are nonequivalent.

The semibridged carbonyl formation is preferred for **3** as this gives each metal 18 electrons. A similar two-isomer cluster has been observed by Gladfelter and co-workers for $[Ru_3CoH_3(CO)_{12}]$.[9] Compounds of **3** and $[Ru_3CoH_3(CO)_{12}]$ appear to be stable toward oxidation both in the solid state and in solution. They differ noticeably from $[Os_3CoH_3(CO)_{12}]$, which is air sensitive.[13] Pertinent spectral data are summarized in Tables 1 and 2.

Experimental Section

General Comments. All reactions and manipulations, except chromatographic separations, were carried out under nitrogen atmosphere using standard Schlenk techniques.[14] The products are not, however, especially sensitive to air.

Infrared spectra were recorded in *n*-hexane on a Nicolet 20SXC FT-IR spectrometer. ^1H and ^{31}P NMR spectra were measured on a Bruker AM-250 spectrometer with $CDCl_3$ or toluene-d_8 as solvent. The ^1H NMR spectra were referenced to external TMS and the ^{31}P NMR spectra were referenced to external 85% H_3PO_4, such that shifts to higher frequencies relative to the reference are taken as positive.

Reagents. $[Ir(CO)Cl(PPh_3)_2]$ (Strem) was of commercial origin and was used without further purification. $[Ru_3(CO)_{12}]$ was prepared from $RuCl_3 \cdot xH_2O$ by a literature method,[15] and the cluster anion $[Ru_3H(CO)_{11}]^-$ was prepared by a published procedure.[16] Tetrahydrofuran (THF) was dried and deoxygenated by stirring over Na/benzophenone ketyl and freshly distilled before use. Other solvents were deoxygenated by bubbling N_2 through them.

Reaction in THF (I). $[Ir(CO)Cl(PPh_3)_2]$ (383 mg, 0.49 mmol) dissolved in 40 mL of THF was mixed with a freshly prepared solution of $Na[Ru_3H(CO)_{11}]$[16] (made from 360 mg, 0.56 mmol of $[Ru_3(CO)_{12}]$) in THF; the Ir/Ru molar ratio was approximately 1:1. The color immediately changed from yellow to dark red. After the solution was stirred for 1 h at room temperature, the solvent was evaporated under vacuum and the solid residue was treated with 85% H_3PO_4. The impurities were removed with hexane, and the residue was extracted with CH_2Cl_2 giving a red solution. The solvent was evaporated under vacuum (yielding 671 mg of solid material), and the residue was chromatographed on a silica column (30 cm). Elution with hexane gave a yellow band of $[Ru_3(CO)_{12}]$ (237 mg, 35%). Further elution with a hexane−dichloromethane (6:1) mixture gave two red bands, which were difficult to separate, and finally elution with a hexane−dichloromethane (4:1) mixture gave a fourth, red band. Since the separation of the fractions was not satisfactory, the second, third, and fourth fractions were reseparated by TLC, with each fraction eluted with a hexane−dichloromethane (6:1) mixture. The second fraction (red) was then identified as **1** (98 mg, 15%). The third fraction (red) contained both **2** (111 mg, 17%) and **3** (57 mg, 9%), and the fourth fraction (red) contained **4** (and **5**) (139 mg, 21%). All products were crystallized from hexane−dichloromethane at 4 °C, and they were characterized by IR and ^1H and ^{31}P NMR.

Compound 1. NMR ($CDCl_3$, 293 K): ^1H (250 MHz), δ 7.43 (m, C_6H_5), −16.9 (dd, Ru−H−Ru), and −17.9 (t, Ru−H−Ru); $^{31}P\{^1H\}$ (250 MHz), δ 35.7 ppm. IR (hexane, cm^{-1}): ν_{CO} 2095 w, 2069 w, 2048 s, 2031 m, 2026 m, 2016 s, and 1988 w. Anal. Calcd for $C_{29}H_{18}Ru_3O_{11}PIr$: C, 32.59; H, 1.70. Found: C, 33.09; H, 1.69.

Compound 2. NMR ($CDCl_3$, 293 K): ^1H (250 MHz), δ 7.44 (m, C_6H_5), and −18.4 (d, Ru−H−Ir); $^{31}P\{^1H\}$ (250 MHz), δ 2.4 ppm. IR (hexane, cm^{-1}): ν_{CO} 2086 m, 2049 vs, 2042 vs, 2031 s, 2009 m, 2000 m, and 1877 w. Anal. Calcd for $C_{30}H_{16}Ru_3O_{12}PIr$: C, 32.91; H, 1.47. Found: C, 33.64; H, 1.99.

Compound 3. ^1H NMR (250 MHz): $CDCl_3$, 293 K, δ 7.49 (m, C_6H_5) and −17.9 (s, br, Ru−H−Ru and Ru−H−Ir); toluene-d_8, 193 K, δ 7.53 (s, C_6H_5), 7.45 (s, C_6H_5), 7.37 (s, C_6H_5), −15.2 (br, Ru−H−Ru), −16.6 (s, Ru−H−Ru), −17.7 (br, Ru−H−Ir), −19.1 (d, Ru−H−Ir), and −21.0 (br, Ru−H−Ru). $^{31}P\{^1H\}$ NMR ($CDCl_3$, 293 K, 250 MHz): δ 34.1 ppm. IR (hexane, cm^{-1}): ν_{CO} 2089 w, 2068 s, 2054 m, 2048 s, 2037 m, 2024 s, 2005 m, 1985 w, and 1961 w. Anal. Calcd for $C_{29}H_{18}Ru_3O_{11}PIr$: C, 32.59; H, 1.70. Found: C, 33.03; H, 1.74.

Compound 4 (and 5). ^1H NMR (250 MHz; $CDCl_3$): 293 K, δ 7.32 (br, C_6H_5), −16.4 (br), and −17.1 (br); 218 K, δ 7.43 (m, C_6H_5), −16.2 (d), −16.5 (br), and −17.9 (d). $^{31}P\{^1H\}$ NMR ($CDCl_3$, 293 K, 250 MHz): δ 35.1 and 2.3 ppm. IR (hexane, cm^{-1}): ν_{CO} 2073 s, 2041 vs, 2023 vs, 2018 s, 1996 w, 1983 m, and 1960 w. Anal. Calcd for $C_{46}H_{32.50}Ru_{2.54}O_{10}P_2Ir_{1.46}$: C, 38.06; H, 2.43. Found: C, 40.75; H, 2.48.

Reaction in THF (II). A separate experiment in THF starting from 66 mg (0.08 mmol) of $[Ir(CO)Cl(PPh_3)_2]$ and $Na[Ru_3H(CO)_{11}]$[16] (prepared from 201 mg, 0.31 mmol, of $[Ru_3(CO)_{12}]$) produced on silica four bands, of which the first band was $[Ru_3(CO)_{12}]$ (96 mg, 46%), characterized by IR, and the fourth band was **4** (and **5**) (49 mg, 23%). The band combined from fractions 2 and 3 was treated with hydrogen to increase the yield of **3**. The chromatographic separation after the hydrogen treatment was carried out on a silica plate with a hexane−dichloromethane (4:1) mixture as eluent. Five fractions were obtained. The first fraction (yellow) was $[Ru_3(CO)_{12}]$, the second fraction (brown) $[Ru_4H_4(CO)_{11}(PPh_3)]$ (14 mg, 7%), the third fraction (yellow) **1** (28 mg, 13%), and the fourth fraction (brown) **3** (21 mg, 10%). The second fraction was crystallized from hexane−dichloromethane at 4 °C. All products were characterized by IR and ^1H and ^{31}P NMR. The fifth fraction was an unidentified compound and attempts to recrystallize it failed.

Compound $[Ru_4H_4(CO)_{11}(PPh_3)]$. NMR ($CDCl_3$, 293 K): ^1H (250 MHz), δ 7.47 (s, C_6H_5), 7.46 (s, C_6H_5), 7.44 (s, C_6H_5), and −17.3 ppm (d, Ru−H−Ru); $^{31}P\{^1H\}$ (250 MHz), δ 38.7 ppm. IR (hexane, cm^{-1}): ν_{CO} 2095 m, 2087 w, 2068 vs, 2059 s, 2050 m, 2028 vs, 2016 m, 2009 m, 1998 w, 1991 w, and 1969 w.

Reaction in THF (III). A new Ru_4 cluster was formed in the reaction of $[Ir(CO)Cl(PPh_3)_2]$ (235 mg, 0.30 mmol) and $Na[Ru_3H(CO)_{11}]$[16] (prepared from 227 mg, 0.36 mmol, of $[Ru_3(CO)_{12}]$) in THF (40 mL). The solution was stirred for 1 h at room temperature. Chromatographic separation on silica with hexane as eluent gave a yellow band of $[Ru_3(CO)_{12}]$ (110 mg, 45%), characterized by IR. Further elution with a hexane−dichloromethane (6:1) mixture gave two red bands (bands 2 and 3), and elution with pure dichloromethane gave a fourth (red) and a fifth (yellow) band. The separated bands were dried under vacuum, and then reseparated by TLC, with each

(13) Wei, C. H. *Inorg. Chem.* **1969**, *8*, 2384.
(14) Shriver, D. F.; Drezdzon, M. A. *The Manipulation of Air-Sensitive Compounds*, 2nd ed.; John Wiley and Sons: New York, 1986.
(15) Eady, C. R.; Jackson, P. F.; Johnson, B. F. G.; Lewis, J.; Malatesa, M.; McPartlin, M.; Nelson, W. J. H. *J. Chem. Soc., Dalton Trans.* **1980**, 383.
(16) Johnson, B. F. G.; Lewis, J.; Raithby, P. R.; Süss, G. *J. Chem. Soc., Dalton Trans.* **1978**, 1356.

Table 6. Summary of Crystallographic Data for Compounds 1−5

	1	**2**	**3**	**4** and **5**
formula	$Ru_3IrC_{29}H_{18}O_{11}P$	$Ru_3IrC_{30}H_{16}O_{12}P$	$Ru_3IrC_{29}H_{18}O_{11}P$	$Ru_{2.5}Ir_{1.5}C_{47}H_{34.5}O_{10}P_2Cl_2$
fw	1068.8	1094.8	1068.8	1429.7
cryst system	triclinic	triclinic	triclinic	triclinic
space group	$P\bar{1}$	$P\bar{1}$	$P\bar{1}$	$P\bar{1}$
a, Å	9.316(2)	9.229(3)	9.073(3)	11.472(3)
b, Å	12.024(3)	11.168(3)	11.853(3)	13.652(3)
c, Å	14.883(5)	16.915(4)	16.574(3)	16.373(4)
α, deg	100.05(2)	103.37(2)	69.32(2)	104.48(2)
β, deg	94.61(2)	96.08(2)	87.50(2)	90.99(2)
γ, deg	90.35(2)	99.88(3)	82.08(3)	96.61(2)
V, Å^3	1651.6(9)	1651.6(8)	1651.6(9)	2463.5(10)
Z	2	2	2	2
D_{calcd}, g cm^{-3}	2.15	2.20	2.15	1.93
cryst dimens, mm	0.15 × 0.30 × 0.50	0.15 × 0.30 × 0.40	0.25 × 0.40 × 0.40	0.10 × 0.25 × 0.50
radiation	Mo Kα	Mo Kα	Mo Kα	Mo Kα
monochromator	graphite	graphite	graphite	graphite
2*θ* limits, deg	4−55	4−55	4−55	4−55
no. of unique reflcns	7564	7621	7632	11362
no. of obsd reflcns	6547	6296	6226	7462
μ(Mo Kα), cm^{-1}	54.2	54.7	54.2	51.5
R [$I > 2\sigma(I)$][a]	0.033	0.053	0.033	0.064
wR[b]	0.040		0.038	
w$R(F^2)$[c]		0.140[d]		0.189[e]

[a] $R = \sum||F_o| - |F_c||/\sum|F_o|$. [b] Weight $= 1/(\sigma^2(F) + 0.0005F^2)$. [c] Weight $= 1/[\sigma^2(F_o^2) + (aP)^2 + bP]$. $P = [(F_o^2) + 2F_c^2]/3$. [d] $a = 0.0934$ and $b = 15.96$. [e] $a = 0.0880$ and $b = 2.57$.

fraction eluted with a hexane−dichloromethane (5:1) mixture. The second fraction (red) was **1** (18 mg, 7%) and the third fraction (red) was **2** (4 mg, <5%), [$Ru_4H_2(CO)_{12}(PPh_3)$] (10 mg, <5%), and **3** (17 mg, 7%). The fourth fraction (red) was **4** (and **5**) (78 mg, 32%). All products were characterized by IR and ^{1}H and ^{31}P NMR. Attempts to recrystallize the fifth fraction failed.

Compound [$Ru_4H_2(CO)_{12}(PPh_3)$]. NMR ($CDCl_3$, 263 K): ^{1}H (250 MHz), δ 7.47 (br, C_6H_5) and −17.8 ppm (br, Ru−H−Ru); ^{31}P{^{1}H} (250 MHz), δ 2.2 ppm. IR (hexane, cm^{-1}): ν_{CO} 2092 w, 2089 sh, 2067 w, 2054 s, 2050 vs, 2039 m, 2029 s, 2013 w, 2003 w, 1998 w, 1989 w, 1981 w, and 1897 m.

Reaction in CH_2Cl_2. [$Ir(CO)Cl(PPh_3)_2$] (236 mg, 0.30 mmol) and a freshly prepared solution of Na[$Ru_3H(CO)_{11}$][16] (made from 275 mg, 0.43 mmol [$Ru_3(CO)_{12}$]) were dissolved in CH_2Cl_2 (50 mL). A color change from yellow to dark red was immediately observed. The Ir/Ru molar ratio was approximately 1:1. After the solution had been stirred for 1 h at room temperature, the unreacted [$Ir(CO)Cl(PPh_3)_2$] was filtered off and the solvent was evaporated from the filtrate under vacuum. The residue was chromatographed on a silica gel column. Elution with hexane gave a yellow band of [$Ru_3(CO)_{12}$] (91 mg, 22%), and further elution with a hexane−dichloromethane (6:1) mixture gave two red bands which were dried under vacuum. One of these was **1** (44 mg, 11%), and the other was **2** (54 mg, 13%). Further elution with a hexane−dichloromethane (1:1) mixture gave two fractions, of which one was **4** (and **5**) (13 mg, <5%) and the other band remained unidentified (59 mg, 14%). Elution with pure dichloromethane gave a small fraction, which also remained unidentified (18 mg, <5%). The products were repurified by TLC, with each fraction eluted separately with a hexane−dichloromethane (6:1) mixture. All products were characterized by IR and ^{1}H NMR. Attempts to recrystallize the fifth and sixth fractions failed.

Reaction in Hexane. [$Ir(CO)Cl(PPh_3)_2$] (138 mg, 0.18 mmol) was reacted with a freshly-prepared solution of Na[$Ru_3H(CO)_{11}$][16] (made from 137 mg, 0.21 mmol, of [$Ru_3(CO)_{12}$]) in hexane (100 mL). The solution was refluxed under stirring for 1 h. As small amount of THF was added to ensure that the starting materials were fully dissolved. A color change from yellow to dark red was immediately observed. The solvent was evaporated under vacuum and the residue chromatographed on a silica column. Elution with hexane gave a yellow band of [$Ru_3(CO)_{12}$] (55 mg, 58%). Further elution with a hexane−dichloromethane (6:1) mixture gave two red bands, one of which was **1** (20 mg, 21%) and the other **2** (7 mg, 7%). Further elution with a hexane−dichloromethane (3:1) mixture also gave two red bands: fractions 4 and 5. Fraction 4 contained compound **4** (and **5**) (10 mg, 11%) and fraction 5 contained an unidentified compound. With pure dichloromethane, yet one more compound was eluted. This also remained unidentified. All products were characterized by IR and ^{1}H NMR. Attempts to recrystallize the fifth and sixth fractions failed.

X-ray Crystallography. Crystals were grown by slow evaporation from saturated CH_2Cl_2/hexane solution. The data for the compounds were collected on a Nicolet R3m diffractometer using Mo Kα radiation ($\lambda = 0.710\ 73$ Å). Accurate cell parameters were obtained from 20−25 centered reflections in the range $15° < 2\theta < 25°$. Intensities were corrected for background, polarization, and Lorentz factors. Empirical absorption corrections were made from ψ-scan data for **1** and **3**. Pertinent crystal and refinement data are listed in Table 6.

The metal atom positions were solved by direct methods with use of the SHELXTL program package.[17] All remaining non-hydrogen atoms were located by the usual combinations of full-matrix least-squares refinement and difference electron density syntheses using SHELXTL[17] for **1** and **3** and SHELXL93[18] for **2** and **4** (and **5**). Metal, phosphorus, oxygen, and carbon atoms were anisotropically refined in all structures. In **4** (and **5**) the disordered dichloromethane solvent molecule was refined isotropically. Phenyl protons were placed in idealized positions (C−H = 0.96 Å, $U = 0.06$ Å^2) and not refined. Hydride ligands of **1** and **3** were located from a difference Fourier map and refined isotropically.

Supporting Information Available: Crystal structure data for compounds **1**−**5**, including tables of positional and thermal parameters, calculated positional parameters for the hydrogen atoms, anisotropic displacement parameters, and complete bond lengths and bond angles (38 pages). Ordering information is given on any current masthead page.

OM960432B

(17) Sheldrick, G. M. *SHELXTL-Plus*, Release 4.11/v; Siemens Analytical X-ray Instruments Inc.: Madison, WI, 1990.
(18) Sheldrick, G. M. *SHELXL93. Program for the Refinement of Crystal Structures*; Univ. of Göttingen: Göttingen, Germany, 1993.